International Journal of Advances in Engineering and Management (IJAEM)
Volume 3, Issue 7 July 2021, pp: 3627-3637 www.ijaem.net ISSN: 2395-5252

Automatic Prediction of Corona virus using Convolutional Neural Network Model

P.Rukmesh[1], K.Rakesh[2], S.G.A.Mounika Lakshmi[3], S.V.N.Jaya Srilakshmi[4], T.Lakshmi Prasanna[5]

[1]*Department of computer Science Engineering, Raghu Institute of Technology, Visakhapatnam, India*
[2]*Assistant Professor, Department Of Computer Science and Engineering, Raghu Institute of Technology, Visakhapatnam, India*
[3]*Department of computer Science Engineering, Raghu Institute of Technology, Visakhapatnam, India*
[4]*Department of computer Science Engineering, Raghu Institute of Technology, Visakhapatnam, India*
[5]*Department of computer Science Engineering, Raghu Institute of Technology, Visakhapatnam, India*

Submitted: 15-07-2021 Revised: 29-07-2021 Accepted: 31-07-2021

ABSTRACT: Currently, the detection of corona virus disease 2019 (COVID-19) is one of the main challenges in the world, given the rapid spread of the disease. Recent statistics indicate that the number of people diagnosed with COVID-19 is increasing exponentially, with more than 1.6 million confirmed cases; the disease is spreading to many countries across the world. We analyse the incidence of COVID-19 spreading across the world. We present an artificial-intelligence technique based on a deep convolutional neural network (CNN) to detect COVID19 patients using real-world datasets.

KEYWORDS: Convolutional Neural Network, Artificial Intelligence Technique, Image Processing, Identification, Diagnosis of Infection,covid-19.

I. INTRODUCTION

The novel coronavirus disease 2019 (COVID-19) pandemic is an on-going pandemic caused by severe acute respiratory syndrome coronavirus 2 (SARS-CoV-2). As of May 2020, more than 5.5 million cases of COVID-19 have been noticed in 216 countries, areas and territories, resulting in 353,373 deaths [Org20]. While most people only have mild to moderate symptoms, some patients have developed severe illnesses that include pneumonia and acute respiratory distress syndrome (ARDS). To control the spreading of COVID-19, effective screening of patients is critical. So far, the gold standard screening method is the reverse transcription polymerase chain reaction (RT-PCR) test which has been designed to detect SARS-CoV-2 genetically. But it only has a positive rate ranging between 30% and 60% [AYH20, YYS]. For patients who develop severe illnesses such as pneumonia and ARDS, a good complementary screening method is radiography examination, where chest radiography imaging (e.g., X-ray or computed tomography (CT) scan) is analysed for SARS-CoV-2 viral infection indicators including bilateral, peripheral ground-glass opacities and pulmonary consolidations [SAB20]. However, the viral infection indicators can be subtle and it is difficult for radiologists to distinguish COVID-19 pneumonia from normal cases or other pneumonias. Thus, computer-aided diagnostic systems that can help detect COVID-19 pneumonia in chest radiography images are highly desired.

In deep learning area, convolutional neural networks (CNN) are typically used to solve object detection and image classification problem due to its ability to preserve spatial structure and recognize image features. LeNet-5 [LBB98], introduced by LeCun et al.in 1998, is the first instantiation of CNN that has been successfully used in practice. With only sevenlayers, it has achieved high performance for digit recognition problem. In 2012, AlexNet [KSH12] entered the ImageNet Large Scale Visual Recognition Challenge (ILSVRC) [RDS15], abenchmark for object detection and image classification tasks at large scale, and was able to outperform all previous non-deep-learning-based models by a significant margin with top-5 error rate at 16.4%. In 2013, ZFNet [ZF14] was designed with the architecture of AlexNet and better hyper parameters. Thus, it reached less top-5 error rate at 11.7%. In 2014, VGGNet [SZ14] and GoogLeNet [SLJ15] both made another jump in performance, with top-5 error rate at 7.3% and 6.7%, respectively. The common thing between VGGNet and GoogLeNet is that they both have deeper architectures. In 2015, the ILSVRC winner is the residual neural network

(ResNet) with 152 layers [HZR16]. It achieved the top-5 error at 3.6% which is less than human error 5.1%. This is the first time that a CNN model outperforms human in large scale object recognition tasks and it marks the promising future for CNN models.

Motivated by the need for fast and accurate analysis of radiography images, a number of COVID-19 pneumonia detection models based on state-of-the-art CNN models have been proposed and results have shown to be promising [CRK20, NKP20, AM20]. However, those studies are reporting the results on small datasets under binary classification (COVID-19 pneumonia and non-COVID-19 cases) or three-class classification (COVID-19 pneumonia, other pneumonias and normal cases) problem. In this study, we have prepared comparatively large dataset consisting chest X-rays images of COVID-19 pneumonia, viral pneumonia, bacterial pneumonia, and normal cases, and have trained two models based on transfer learning concept and ResNet architecture. One model is trained to distinguish COVID-19 pneumonia and non-COVID-19 cases in chest X-ray images, while the other one is trained to classify COVID-19 pneumonia, viral pneumonia, bacterial pneumonia, and normal cases. Using the first model, we can quickly screen patients who are suspected of having COVID-19 pneumonia and arrange immediate medical cares for them. The second model can help clinicians to not only better screen COVID-19, but also decide treatment strategy and make treatment plan based on cause of the infection.

This thesis is organized as. First, Chapter 2 describes the generation of datasetfor two models. Chapter 3 describes the model architecture, transfer learning concept, implementation details, performance evaluation metrics, and the model interpretation strategy. Chapter 4 presents and discusses the results of experiments conducted to evaluate and interpret the proposed models. Finally, conclusions are drawn in C.

II. LITERATURE SURVEY

In addition to classify COVID-19 and normal cases, Hu et al. [10] performed another experiment to differentiate COVID-19 cases from other cases as bacterial pneumonia and SARS. The average sensitivity, specificity, and the AUC score were obtained as 0.8571, 84.88%, and 92.22%, respectively.

Baietal.implemented the deep learning architecture EfficientNet B4 to classify COVID-19 and pneumonia slices of CT scans. The diagnoses of the six radiologists on the corresponding patients were used to evaluate the efficiency of the results obtained by an AI model. The AI model achieved 96% of accuracy, while the average accuracy of the diagnosis of radiologists was obtained at 85%.

Kang et al. proposed a pipeline and multiview representation learning technique for COVID-19 classification using different types of features extracted from CT images. They used 2522 CT images (1495 are from COVID-19 patients, and 1027 are from community- acquired pneumonia) for the classification purpose. The comparison was performed using the benchmark machine learning models, namely, support vector machine, logistic regression, Gaussian-naive-Bayes classifier, K-nearest- neighbours', and neural networks. The proposed method outperformed the considered ML models with 95.5%, 96.6%, and 93.2% in terms of accuracy, sensitivity, and specificity, respectively.

Other study was performed by Shi et al. to classify COVID-19 and pneumonia. They considered 1658 and 1027 confirmed COVID-19 and CAP cases. Shi et al. proposed a model that is based on random forest and automatically extracted a series of features as volume, infected lesion number, histogram distribution, and surface area from CT images. The proposed method and considered machine learning models like logistic regression, support vector machine, and neural network were then trained by the selected features with 5-fold crossvalidation. The authors reported that the proposed method outperformed other models and produced the optimal AUC score (0.942).

Ying et aldesigned a network named as DRE-Net, which is based on the modifications on pretrained ResNet-50. The CT scans of 88 COVID-19 confirmed patients, 101 patients infected with bacteria pneumonia, and 86 healthy persons. The designed network was compared by the pre- trained models, ResNet, DenseNet, and VGG16. The following results showed that the designed network out performed other models by achieving 0.92 and 0.95 of AUC scores for the image and human levels.

In addition to COVID-19/non-COVID-19 classification, Han et al. performed experiments to classify COVID-19, common pneumonia, and no pneumonia cases as three classes classification. Their proposed AD3D-MIL model achieved accuracy, AUC, and the Cohen kappa score of 94.3%, 98.8%, and 91.1%, respectively.

Ko et al.proposed a model, a fast-track COVID-19 classification network (FCONet) that used VGG16, ResNet- 50, InceptionV3, and Xception as a backbone to classify images as COVID-19, other pneumonia, or no pneumonia.

International Journal of Advances in Engineering and Management (IJAEM)
Volume 3, Issue 7 July 2021, pp: 3627-3637 www.ijaem.net ISSN: 2395-5252

They've considered 1194 COVID-19, 264 low-quality COVID- 19 (only for testing), and 2239 pneumonia, normal, and other disease CT scans in their observation. All images were converted into grayscale image format with dimensions of 256 × 256. They used rotation and zoom data augmentation procedures to maximize the number of training samples. It was concluded that FCONet based on ResNet-50 outper- formed other pretrained models and achieved 96.97% of accuracy in the external validation data set of COVID-19 pneumonia images.

Li et al. [8] proposed a COVNet that used ResNet50 as a backbone to diff erentiate COVID-19, nonpneumonia, and community-acquired pneumonia.4352 chest CT scans from 3322 patients were considered for their study. A max- pooling operation was applied to the features obtained from COVNet using the slices of the CT series, and the resultant feature map was loaded to a fully connected layer. This led to generate a probability score for each considered class. It was concluded that the proposed model achieved a sensitivity, specificity, and ROC AUC scores of 90%, 96%, and 0.96, respectively, for the COVID-19 class.

Ni et alconsidered a total of 19,291 CT scans from 14,435 individuals for their proposed model to detect COVID-19 in CT scans. The proposed model included Multi-View Point Regression Networks (MVPNet), 3D UNet, and 3D UNet-based network for lesion detection, lesion segmentation, and lobe segmentation, respectively. Their algorithm analysed the volume of abnormalities and the distance between lesion and pleura to diagnose the COVID-19, and it was concluded that the proposed algorithm outperformed three radiologists in terms of accuracy and sensitivity by achieving 94% and 100%, respectively. Table 3 summarizes the classification results for COVID-19/non-COVID-19 pneumonia cases.

COVID-19 Severity Classification Studies. Xiao et al. implemented a pretrained network ResNet34 to diagnose COVID-19 severity. The experiments were performed using five-fold cross-validation, and 23,812 CT images of408 patients were considered. They concluded that the model achieved the ROC AUC score of 0.987, and the prediction quality of detecting severity and no severity of 87.50% and 78.46%.

Zhu et alproposed a model which was optimized by traditional CNN and VGG16 to stage the COVID-19 severity. A publicly available dataset was considered, and 113 COVID-19 confirmed cases were used to test their hypothesis. Obtained scores were compared by scores given by radiologists, and it was concluded that the top model achieved a correlation coefficient (R2) and mean absolute error of 0.90 and 8.5%, respectively.

Pu et al. proposed an approach that initially segmented lung boundary and major vessels at two points using UNet and registered these two images using a bidirectional elastic registration algorithm. Then, the average density of the middle of the lungs was used to compute a threshold to detect regions associated with pneumonia. Finally, the radiologist used to rate heat map accuracy in representing progression.Two datasets that consisted of 192 CT scans were considered in their study. Table 4 summarizes the key findings of the severity quantification studies.

Table 3: COVID-19/non-COVID-19 pneumonia classification results. Class.: classification; bac. pneu.: bacterial pneumonia; Sens.: sensitivity; Spec.: specificity; Prec.: precision; Acc.: accuracy; AUC: area under the curve; Ref.: reference.

Class.	Subjects	Dataset	Method	Sens. (%) or recall	Spe. (%)	Pre. (%)	Acc (%)	AUC (%)	F1-score	Ref.
COVID-19/influ-A/normal	219 COVID-19 224 influ-A 175 normal	Private	CNN ResNet	86.7	N/A	81.3	N/A	N/A	83.9	Xu et al. [52] Peer-reviewed
COVID-19/CT-EGFR	1266 COVID-19 4106 CT-EGFR	Private	COVID19Net (DenseNet-like str.)	79.35	71.43	N/A	85.00	86.00	90.11	Wang et al. [53] Peer-reviewed
COVID-19/other pneu.	521 COVID-19 397 normal 76 bac. pneu. 48 SARS	[26, 47]	DL EfficientNet V2	85.71	84.88	N/A	85.40	92.22	N/A	Hu et al. [10] Preprint
COVID-19/other pneu.	521 COVID-19 665 non-COVID-19 pneu.	Private	DNN EfficientNet B4	95	96	N/A	96	95	N/A	Bai et al. [54] Peer-reviewed
COVID-19/CAP	1495 COVID-19 1027 CAP	Private	Multiview representation learning	96.6	93.2	N/A	95.5	NA	N/A	Kang et al. [56] Peer-reviewed
COVID-19/CAP	1658 COVID-19 1027 CAP	Private	RF-based ML model	90.7	83.3	N/A	87.9	94.2	N/A	Shi et al. [57] Preprint
COVID-19/bac. pneu./normal	88 COVID-19 101 bac. pneu. 86 normal	Private	DRE-Net	96	N/A	79	86	95	87	Ying et al. [58] Preprint
COVID-19/other pneu./non-pneu.	230 COVID-19 100 normal	Private	AD3D-MIL	90.5	NA	95.9	94.3	98.8	92.3	Han et al. [44] Peer-reviewed
COVID-19/other pneu./non-pneu.	1194 COVID-19 1357 other pneu. 998 normal 444 lung cancer	Private + [26, 47]	FCONet ResNet50	99.58	100.0	NA	99.87	100.0	NA	Ko et al. [59] Peer-reviewed
COVID-19/other pneu./non-pneu.	1296 COVID-19 1735 pneumonia 713 non-pneu.	Private	COVNet ResNet50	90	96	NA	NA	96.0	NA	Li et al. [8] Peer-reviewed
COVID-19/other pneu./healthy	3854 COVID-19 6871 other pneu. 8566 healthy	Private	MVPNet 3D UNet 3D UNet-based network	100	25	NA	94	NA	97.0	Ni et al. [60] Peer-reviewed

tional and Mathematical Methods in Medicine

International Journal of Advances in Engineering and Management (IJAEM)
Volume 3, Issue 7 July 2021, pp: 3627-3637 www.ijaem.net ISSN: 2395-5252

III. PROBLEM STATEMENT

In Most of the Existing System a support vector machine (SVM) model and resnet50 model for the classification of patients with COVID-19 and other types of pneumonia using CT chest images. This was done by extracting textural and histogram features of the infections and obtaining a radionics features vector from each sample.

IV. OBJECTIVE

To develop an artificial-intelligence tool based on a deep convolution neural network (CNN) which can examines chest X-ray images to identify such Covid patients which will be available quickly and at low costs.

V. METHODOLOGY

5.1 pre-processing

A set of noise-removal functions accompanied with morphological operations that result in clear image of chest CT scan image after passing through high pass filter is the basic idea behind the proposed algorithm. TheSet of morphological operations used will decide the clarity and quality of the chest CT scan image. After the original image undergoes pre-processing transformations these basic pre-processing transformations include:

1. Altering the image to grayscale, as we need to find contour of the final image which works on grayscaleimages.
2. Applying low pass filter, to remove any noise, if present, in the image.
3. Applying high pass filter, to obtain exact sharpened image with clear-defined boundaries.

5.2 Segmentation

The K-means clustering algorithm. The main idea of this approach is to assign each point or data to a cluster whose centre (centroid) is the closest. The centre of each cluster is the average of all the points in this cluster classification we define a class for the black background of the image with cerebrospinal fluid, a second class for white matter and a third class for grey matter.

5.3 Deep learningnetwork

In this module we build a model of deep learning architecture which consist 16 and 32 Convolutions layer with filter mask and padding filter and Maxpooling layer with filter mask size of 3*3*16 and 3*3*32. The proposed deep learning network is focused on the chest components (grey and white matter) for healthy and unhealthy cases

5.4 Chest abnormalities classification

In these modules all chest components segmented are classified as normal or abnormal cases according to the deep learning network.

In this chapter, we will discuss the model architecture, transfer learning concept, implementation details, performance evaluation metrics, and the strategy for interpreting models.

5.5 ResNet Architecture

Residual neural network (ResNet) is proposed by He et al. in 2015 [HZR16]. The hypothesis behind ResNet is that deeper networks are harder to optimize, since the deeper model should be able to perform as well as the shallower model by copying the learned parameters from the shallower model and setting additional layers to identity mapping. To help optimize deeper models, residual blocks are designed to fit a residual mapping F (x) instead of the desired underlying mapping H(x), and full ResNet architecture is built by stacking residual blocks. More specifically, every residual block has two 3 × 3 convolutional layers. Periodically, the numbers of filters are doubled and spatial down sampling is operated. Figure 3.1 illustrates the structure within the residual block and Figure 3.2 shows an example of ResNet architecture - ResNet with 18 layers (ResNet18).

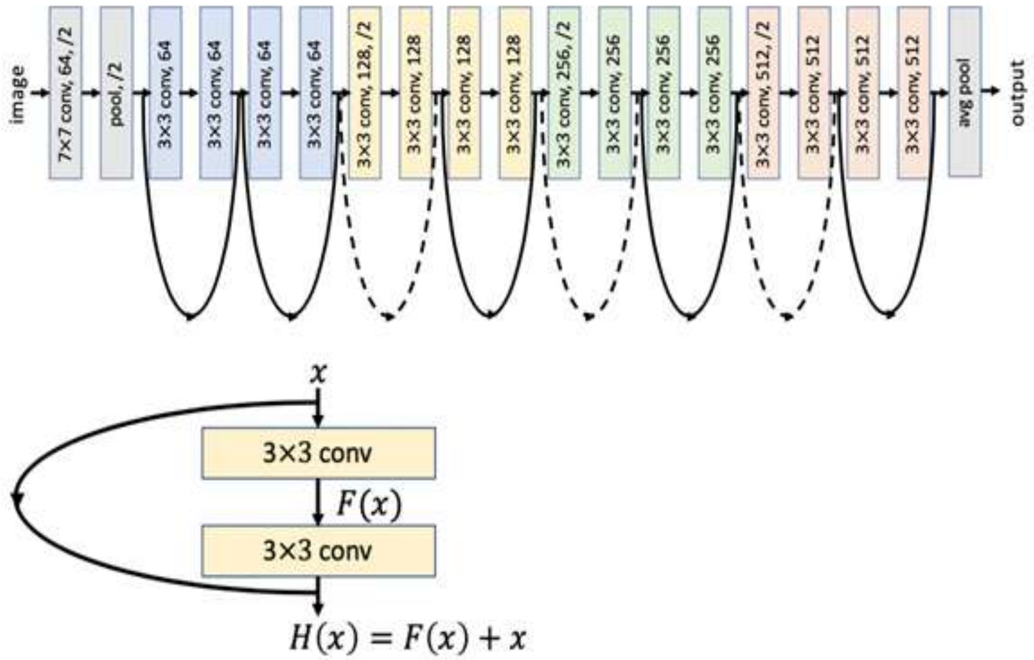

Figure3.2:SchemaofResNet18architecture

In this study, we build two deep models based on ResNet18 for the classification undertwo schemes.One is a binary classification that distinguishes COVID-19 pneumonia andnon-COVID-19 cases, while the other is a four-class classification that classifies COVID-19pneumonia, viralpneumonia, bacterialpneumonia,andnormal

5.6 TransferLearning

A successful training of deep neural networks often requires a large-scale dataset and a long training period. Moreover, a basic assumption for many deep learning models is that the training and testing data should be drawn from the same distribution. In many real-word applications, the availability of data is limited due to the high cost of collecting and labeling data. In such cases, retaining and reusing previously learned knowledge for a different data distribution, task or domain is critical. Transfer learning is a machine learning method where a previously trained model is reused as a starting point for the new model and task. It can not only alleviate the need and effort to collect training data, but also accelerate training process.

There are two commonly used strategies to exploit transfer learning on deep convolutional neural network. The first strategy is called feature extraction where the pretrained model, retaining both its initial architecture and the learned parameters, is only used to extract image features for the input of the new classification model. The second strategy makes some modifications to the pretrained model, such as architecture adjustments and parameter tuning, to improve extracted image features on the new dataset and achieve optimal results.

The second strategy is used in this. More specifically, we use ImageNet[RDS15], a large-scale dataset consisting 1.2 million high-resolution images in 1,000 different classes (i.e. Fish, bird, tree, flowers, sport, room, etc.), to pretrain ResNet18. Since images in ImageNet are different from our dataset, we cannot directly use the pretrained model to extract image features for classification. Instead, we need to fine-tune parameters of the pretrained model on our dataset to generate better image features. Besides, the architecture of ResNet18 has been changed - the number of outputs in the final fully-connected layer is changed from 1,000 to the number of classes in each classification problem. Thus, the fine-tuned model outputs scores for each class and can classify input image to the class with maximum score.

5.7 ImplementationDetails
Data Augmentation

We apply data augmentation methods that include rotation, scaling, translation, and horizontal

International Journal of Advances in Engineering and Management (IJAEM)
Volume 3, Issue 7 July 2021, pp: 3627-3637 www.ijaem.net ISSN: 2395-5252

flip on the training set to address the data deficiency problem. That means, each image in the training set is randomly operated by the following methods:

- **Rotation**: Rotating the image with an angle between 0 and 15 in the clockwise or counter clockwise direction.
- **Scaling**: Sampling the scale of frame size of the image randomly between 90% and 110%.
- **Translation**: Translating image horizontally and vertically between -10% and 10%.
- **Horizontal Flip**: Horizontally flipping the image with a probability of 0.5.

5.8 Hyper parameters

In this study, all images are normalized and resized to 224 × 224 pixels. We use five-fold cross validation to evaluate the model and tune the hyperparameters, and obtain the generalized results in the testing stage. The following hyperparameters are used for training.

Binary classification model: Batch size = 256, cross entropy loss, stochastic gradient descent (SGD) optimizer with momentum = 0.9 and weight decay (L2 penalty) = 0.01, learning rate = 0.003 (will decay by 0.1 at 10 and 20 epoch), 50 epochs in total, and early stopping with patience = 10.

Four-class classification model: Batch size = 256, cross entropy loss, SGD optimizer with momentum = 0.9 and weight decay (L2 penalty) = 0.1, cross entropy loss, learning rate = 0.003 (will decay by 0.1 at 20 and 40 epoch), 50 epochs in total, and early stopping with patience = 15.

5.9 Performance Evaluation Metrics

Due to the data imbalance problem, the performance of the model is evaluated using eight evaluation metrics - accuracy, confusion matrix, precision, recall (or sensitivity), specificity (or selectivity), F1-score, receiver operating characteristic (ROC) curve and area under the curve (AUC).

5.10 Confusion Matrix

A confusion matrix is a summary of predicted labels and true labels on a classification problem. It gives us insights not only into the errors but also into the types of errors that are being made by the classifier. The schema of confusion matrix in a binary classification problem is shown in Figure 3.4.

		Predicted Label	
		Positive	Negative
True Label	Positive	True Positive (TP)	False Negative (FN)
	Negative	False Positive (FP)	True Negative (TN)

Figure3.4:Schemaofconfusionmatrix

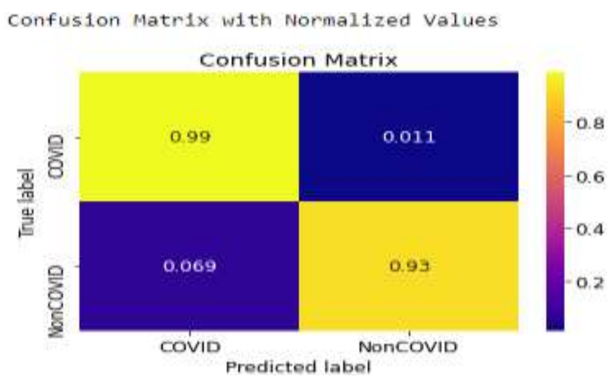

The accuracy, precision, recall (or sensitivity), specificity (or selectivity) and F1-score can be computed as follows based on the confusion matrix.

$$\text{Accuracy} = \frac{TP + FN}{TP + FP + TN + FN}$$

$$\text{Precision} = \frac{TP}{TP + FP}$$

$$\text{Recall (or sensitivity)} = \frac{TP}{TP + FN}$$

$$\text{Specificity (or selectivity)} = \frac{TN}{TN + FP}$$

$$\text{F1-score} = \frac{2 \times \text{precision} \times \text{recall}}{\text{precision} + \text{recall}}$$

ROCCurve

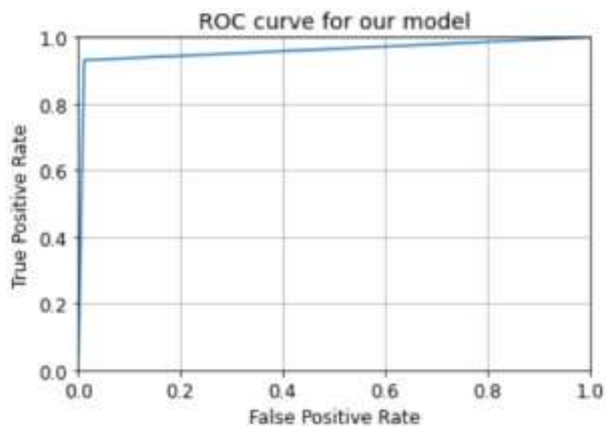

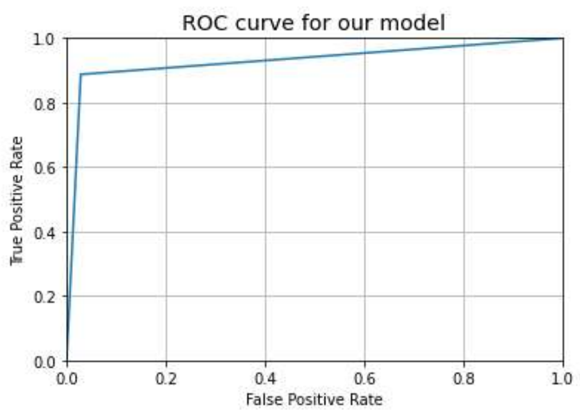

VI. IMPLEMENTATION

6.1 PREPROCESSING:

Most appropriate input data has been selected, it must be pre-processed otherwise, and the neural network will not produce accurate result. This decreases the number of inputs to the network and making it learn more easily. It removes unnecessary signals from the CT images. It converts the color images to grey-level coding.

6.2 RECURRENT NEURAL NETWORK

Performance of the RNN classifier was

evaluated in terms of training performance and classification accuracies. This network is a type of radial basis network and It gives quick and accurate classification and is a promising tool for classification of the defects from quality material. Existing weights will never be changed but only new vectors are inserted into weight matrices when training. So it can be used in real-time. Since the training and running procedure can be implemented by matrix manipulation, the speed of RNN is very fast.

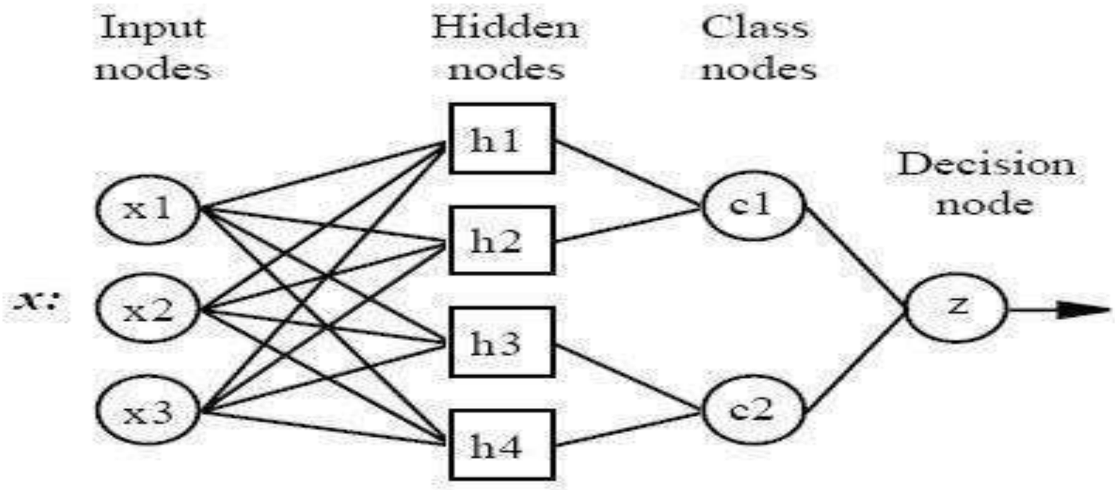

6.3 Architecture of Recurrent Neural Network LAYERS

RNN is often used in classification problems. When an input is present, the first layer computes the distance from the input vector to the training input vectors. This produces a vector where its elements show how close the input is to the training input. The second layer sums the contribution for each class of inputs and produces its net output as a vector of probabilities. Finally, a complete transfer function on the output of the second layer picks the maximum of these probabilities, and produces a 1 (positive identification) for that class and a 0 (negative identification) for non-targeted classes.

- **INPUT LAYER**

Each neuron in the input layers shows a predictor variable. In categorical variables, N-1 neurons are used when there are N numbers of categories. It standardizes the range of the values by subtracting the median and dividing by the inter quartile range. Then the input neurons feed the values to each of the neurons in the hidden layer.

- **PATTERN LAYER**

This layer consists of one neuron for each case in the training dataset. It stores the values of the predictor variables for the case along with the target value. A hidden neuron computes the Euclidean distance of the test case from the neuron's center point and then applies the radial basic function kernel function using the sigma values.

- **SUMMATION LAYER**

For RNN networks there is one pattern neuron for each category of the target variable. The actual target of each training case is stored with each internal (hidden) neuron; the weighted value coming out of a hidden neuron is fed only to the pattern neuron that corresponds to the hidden neuron's category. The pattern neurons add the values for the class they represent.

6.4 CONVOLUTIONAL NEURAL NETWORK

A Convolutional Neural Network (ConvNet/**CNN**) is a Deep Learning algorithm which can take in an input image, assign importance (learnable weights and biases) to various aspects/objects in the image and be able to differentiate one from the other.

International Journal of Advances in Engineering and Management (IJAEM)
Volume 3, Issue 7 July 2021, pp: 3627-3637 www.ijaem.net ISSN: 2395-5252

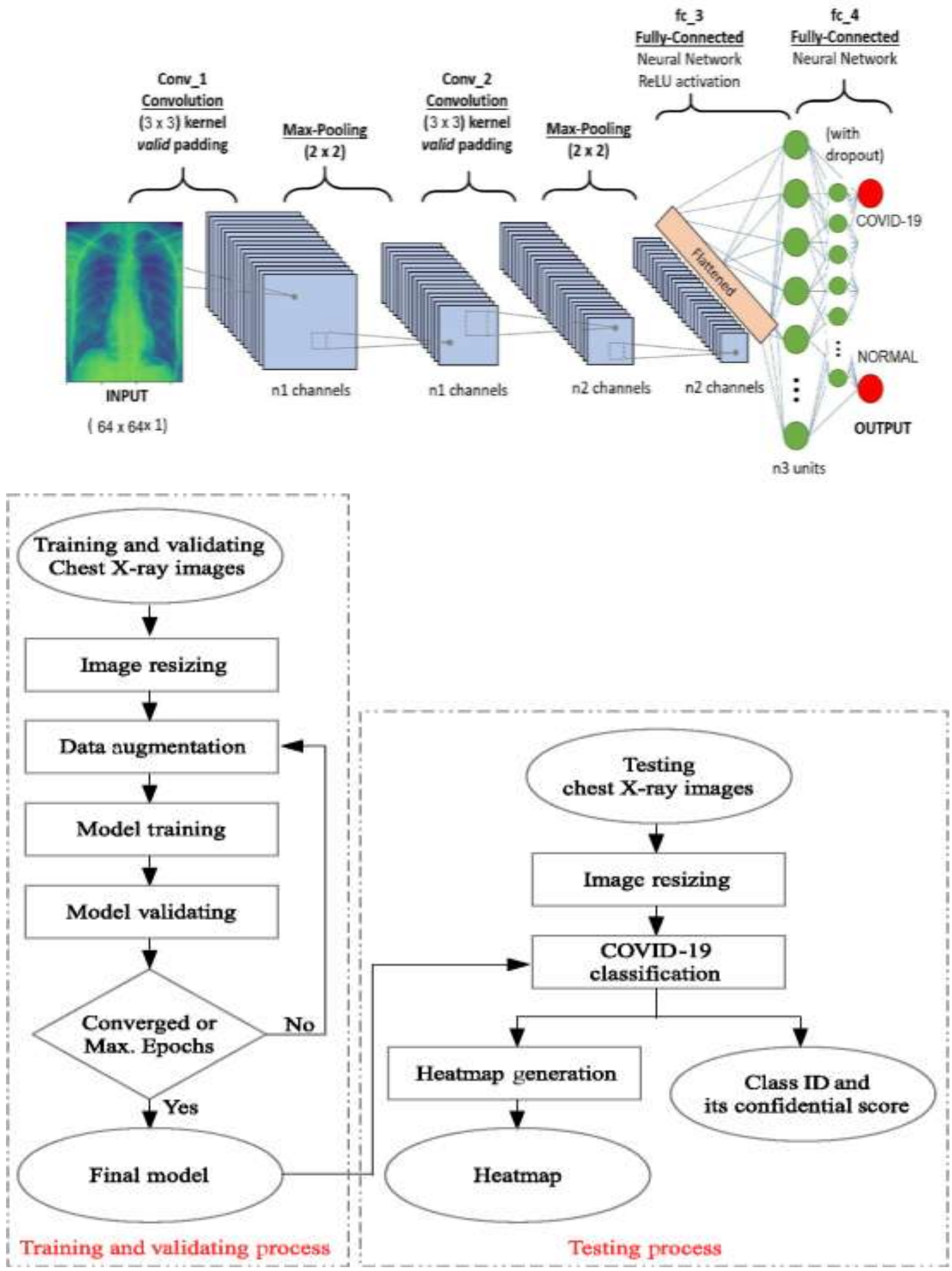

BLOCK DIAGRAM OF PROPOSED SYSTEM

International Journal of Advances in Engineering and Management (IJAEM)
Volume 3, Issue 7 July 2021, pp: 3627-3637 www.ijaem.net ISSN: 2395-5252

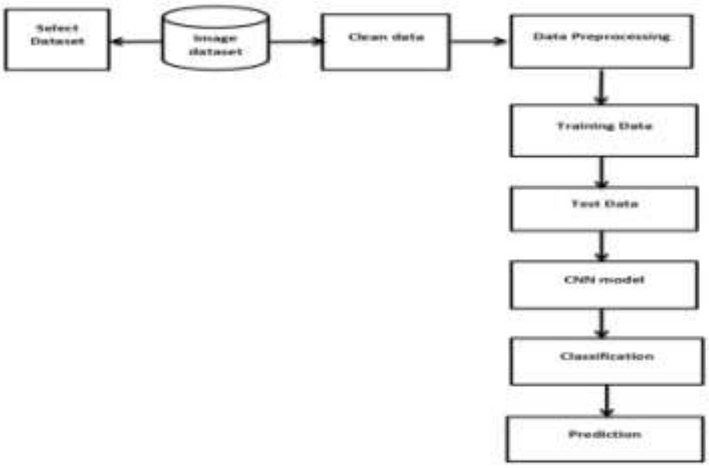

VII. CONCLUSION AND RESULTS

This study shows the feasibility of building a computer-aided diagnostic system that can help clinicians detect COVID-19 pneumonia from radiology images accurately and quickly. Moreover, model interpretation techniques allow us to further evaluate and understand models. However, the limited data adds challenge to the performance of model

By collecting more chest X-ray images of COVID-19 pneumonia, other pneumonias and normal cases, the model will be more robust and powerful.

SUBJECT	DATASET	METHOD	PRECISION	RECALL	F1 SCORE(%)	ACCURACY(%)	REFERENCE(%)
Covid 19	Private	Resnet50	n/a	87.2	n/a	88	Ahuja et .al
Covid 19	Private	Cnn	n/a	86.8	85.6	90	Jin sartum
Covid 19	Not clear	Svm	89.62	90.4	84.3	91	Barsstugan et.al
Covid 19	Chest ct &x-ray	Cnn	92.2	99.9	96.4	96	

REFERENCES

[1]. World Health Organization August 2020, https://www.who.int/emergencies/diseases/novel-coronavirus-2019.

[2]. WorldometerAugust 2020, https://www.worldometers.info/coronavirus/.

[3]. F. Shi, J. Wang, J. Shi et al., "Review of artificial intelligence techniques in imaging data acquisition, segmentation and diagnosis for COVID-19," IEEE Reviews in Biomedical Engi- neering, 2020.

[4]. H. Bai, B. Hsieh, Z. Xiong et al., "Performance of radiologists in differentiating COVID-19 from viral pneumonia on chest CT," Radiology, vol. 296, no. 2, pp. E46–E54, 2020.

[5]. Y. Fang, H. Zhang, J. Xie et al., "Sensitivity of chest CT for COVID-19: comparison to RT-PCR," Radiology, vol. 296, no. 2, pp. E115–E117, 2020.

[6]. S. S. Hare, A. N. Tavare, and V. Dattani, "Validation of the British Society of Thoracic Imaging guidelines for COVID-19 chest radiograph reporting," Clinical Radiology, vol. 75, no. 9,2020

[7]. F. Pesapane, M. Codari, and F. Sardanelli, "Artificial intelligence in medical imaging: threat or opportunity? Radiologists again at the forefront of innovation in medicine," European Radiology Experimental, vol. 2, no. 1, 2018.

[8]. L. Li, L. Qin, Z. Xu et al., "Using Artificial intelligence to Detect COVID-19 and Community-acquired pneumonia Based on Pulmonary CT: Evaluation of the Diagnostic Accuracy," Radi- ology, vol. 296, no. 2, pp. E65–E71, 2020.

[9]. M. Z. Alom, M. M. S. Rahman, M. S. Nasrin, T. M. Taha, and V.K. Asari,

"COVID MTNet: COVID-19 detection with multi-task deep learning approaches," arXiv preprint arXiv, 2004, https://arxiv.org/abs/2004.03747.

[10]. R. Hu, G. Ruan, S. Xiang, M. Huang, Q. Liang, and J. Li, "Auto- mated Diagnosis of COVID-19 Using Deep Learning and Data Augmentation on Chest CT," medRxiv, 2020, https://medRxiv .org/abs/2020.04.24.20078998.

[11]. N. Ma, X. Zhang, H. Zheng, and J. Sun, "ShuffleNet V2: practical guidelines for efficient CNN architecture design," Computer Vision – ECCV 2018: 15th European Conference, Munich, Germany, September 8–14, 2018, Proceedings, Part XIV, Springer International Publishing, vol. 11218, pp. 122– 138, 2018.

[12]. O. Gozes, M. Frid-Adar, H. Greenspan et al., "Rapid AI development cycle for the coronavirus (COVID-19) pandemic: ini- tial results for automated detection & patient monitoring using deep learning CT imag e a nalysis, " arXiv , 2020, https://arXiv:2003.05037.

[13]. H. Kassani, P. H. K. Sara, M. J. Wesolowski, K. A. Schneider, and R. Deters, "Automatic detection of coronavirus disease (COVID-19) in X-ray and CT images: a machine learning based approach," arXiv, vol. 10641, 2004.

[14]. M. Sandler, A. Howard, M. Zhu, A. Zhmoginov, and L.C. Chen, "MobileNetV2: inverted residuals and linear bottle- necks," in 2018 IEEE/CVF Conference on Computer Vision and Pattern Recognition, pp. 4510–4520, Salt Lake City, UT, USA, 2018.

[15]. G. Huang, Z. Liu, L. Van Der Maaten, and K. Weinberger, "Densely connected convolutional networks," in Proceedings of The Ieee Conference On Computer Vision And Pattern Recognition, pp. 4700–4708, Honolulu, HI, USA, 2017.

[16]. F. Chollet, "Xception: deep learning with depth wise separable convolutions," in 2017 IEEE Conference on Computer Vision and Pattern Recognition (CVPR), pp. 1800–1807, Honolulu, HI, USA, 2017.

[17]. C. Szegedy, V. Vanhoucke, S. Ioff e, J. Shlens, and Z. Wojna, "Rethinking the inception architecture for computer vision," in 2016 IEEE Conference on Computer Vision and Pattern Recognition (CVPR), pp. 2818–2826, Las Vegas, NV, USA, 2016.

[18]. C. Szegedy, S. Ioff e, V. Vanhoucke, and A. Alemi, "Inception- v4, inception-ResNet and the impact of residual connections on learning, AAAI'17," in Proceedings of the Thirty-First AAAI Conference on Artificial Intelligence, pp. 4278–4284, San Fran- cisco, CA, USA, 2017.

[19]. K. He, X. Zhang, S. Ren, and J. Sun, "Deep residual learning for image recognition," in 2016 IEEE Conference on Computer Vision and Pattern Recognition (CVPR), pp. 770–778, Las Vegas, NV, 2016.

[20]. A. Jaiswal, N. Gianchandani, D. Singh, V. Kumar, and M. Kaur, "Classification of the COVID-19 infected patients using DenseNet201 based deep transfer learning," Journal of Biomolecular Structure & Dynamics, pp. 1–8, 2020.

[21]. J. P. Cohen, P. Morrison, L. Dao, K. Roth, T. Q. Duong, and M.Ghassemi,"Covid-19 image data collection," arXiv, vol. 11988, 2006https://github.com/ieee8023/covidchest x-ray dataset.

[22]. Kaggle,"RSNA Pneumonia Detection Challenge," 2020, https://www.kaggle.com/c/rsna-pneumonia-detection- challenge.

[23]. Kaggle, "SARS-COV-2 CT-Scan Dataset," https://www.kaggle.com/plameneduardo/sar scov2-ctscan-dataset.

[24]. K. Hun and R. Wen, "COVID19 Dataset," https://github.com/ KevinHuRunWen/COVID-19.

[25]. https://github.com/UCSD-AI4H/COVID-CT.

[26]. COVID-19 Database, "Italian Society of Medical and Interventional Radiology (SIRM)," https://www.sirm.org/en/category/ articles/covid-19-database/.

[27]. ChainZhttp://www.ChainZ.cn.

[28]. S. G. Armato, G. McLennan, L. Bidaut et al., "The lung image database consortium (LIDC) and image database resource initiative (IDRI): a completed reference database of lung nodules on CT scans," Medical physics, vol. 38, no. 2, pp. 915–931, 2011.

[29]. Kaggle,"ChestXRayImages(Pneumonia)data set,"2020,https://www.http://kaggle.com/pau ltimothymooney/chest- xray-pneumonia.

[30]. C. Jin, W. Chen, Y. Cao et al., "Development and evaluation of an AI system for COVID-19 diagnosis," MedRxiv, 2020, https://medRxiv.org/abs/2020.03.20.200398 34. iv.org/ abs/2020.03.19.20039354.nd covid-19 pneumonia?arXiv pre- print arXiv," vol. 13145, 2003.